S REETHU, et al, International Journal of Computers, Electrical and Advanced Communication Engineering [IJCEACE]™. Thomson Reuters (WOS) Research ID: D-1150-2018, Volume 10, Issue 19, PP: 68 - 75, JAN - JUL' 2021

BIDIRECTIONAL PARTIAL POWER CONVERTER INTERFACE FOR ENERGY STORAGE SYSTEMS TO PROVIDE PEAK SHAVING IN GRID-TIED PV PLANTS

S REETHU 1*, B PARASURAM 2

1.M.Tech – Power Systems , 2. Asst. Professor
Dept of EEE

BHEEMA INSTITUTE OF TECHNOLOGY AND SCIENCE, ADONI.

ABSTRACT:

The ever growing participation of modern renewable resources in electric markets has shaken the paradigm of generation-demand constant match. Most modern renewable add intermittent behavior and high variability to electric markets, forcing other renewable and themselves to perform power curtailment and/or having extra generating units connected to the network to compensate power, voltage and frequency variations. In order to handle this scenario, Energy Storage Systems (ESSs) have risen as enabling technologies capable to provide backup energy to compensate power, voltage and frequency fluctuations and, at the same time, offer additional benefits as ancillary services, peak shaving, load shifting, base load generation, etc. This paper presents a novel bidirectional Partial Power Converter (PPC), as an interface between a Battery ESS (BESS) and a grid tied Photovoltaic (PV) plant. To obtain a better understanding of the converter, its mathematical model is presented and its operation modes are explained. The main purpose of this configuration is to provide peak shaving capability to a grid-tied PV plant, while providing a high efficiency BESS. Simulation results show the operation of the full system (grid-tied PV plant and BESS), performing peak shaving under a step-down and up in solar irradiation.

INTRODUCTION

Wind and PV energy have been at the forefront of renewable integration [1]. During the last decades electric markets have experience an immense growth in participation of (traditional and modern) renewable resources, where modern renewables have reached an impressive 10.2% [2]. This has been mostly motivated by government politics, environmental concerns and fossil fuel depletion [3]. High variability and intermittency of modern renewables have set a virtual limit to renewables participation share in electric markets, since highly variable systems require back-up energy generation [4]–[6]. Nowadays, the mainstream solution to deal with generation-demand mismatches is to have spinning-reserves [5], i.e. sets of back up fast-response costly fossil fuel based generating systems, which must be kept operating idle or at low power level. ESSs have been vastly researched as an alternative to deal with generation-demand mismatch and provide additional services [6]–[10]. In [6], the addition of ESSs to

Wind farms in order to perform peak shaving is analyzed. Where an ESS sizing strategy based on Homogeneous Markov Chain, considering wind-storage reliability and increasing the income, is proposed. In [7], the addition of BESS to perform peak shaving in a grid-tied network composed of several loads and PV generation is proposed. The sizing of the BESS considers different pricing strategies, probabilistic neural network forecasting of the behavior of the load and PV generation. In [8], [9], the addition of super capacitor based ESS is considered to perform global maximum power point tracking in a central inverter PV plant, while complying grid code restrictions on maximum power variation per minute. The addition of a BESS to an islanded wind-diesel-loads power sysatem is analysed in [10], where the BESS provides peak shaving and frequency regulation capabilities. A paramount part of adding ESSs to a system is choosing the proper Energy Storage Device (ESD) for the application among several different technologies, namely Pumped Hydro Storage, Compressed Air Energy Storage, Flywheel, Fuel Cell, Rechargeable Batteries, Super Capacitor, etc. There have been some studies comparing ESDs features, for instance, in [11] price, energy density, power density, specific power, specific energy, discharge/charge rate, life cycle, depth of discharge, lifespan, energy conversion efficiency, daily self-discharge rate,and ramp time of several ESDs, to provide uninterruptible power supply to data centres, are presented. A deeper comparison of ESDs is presented in [12], where several ESDs are numerically analyzed presenting their specific energy, energy density, specific power, power density, efficiency, lifespan, life cycle, life cycle, daily self-discharge rate and scale, cost. Efficiency is a topic of great importance when analyzing power systems and even more when analyzing ESDs, since its bidirectional power flow nature incurs in losses during both energy conversion processes (storing and releasing energy). In order to quantify those losses, table I summaries the energy conversion efficiency and daily self-discharge rate of several ESDs.

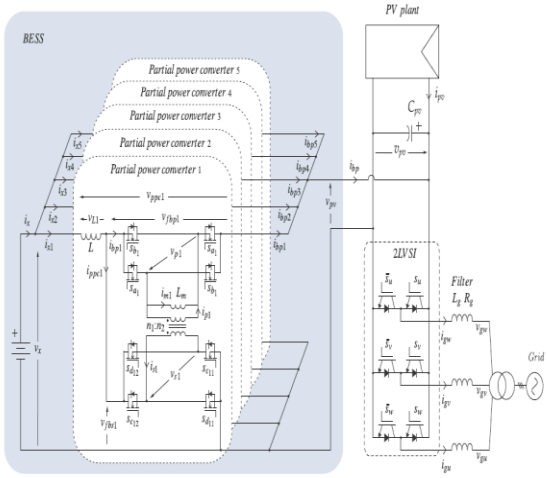

Fig. 1. Proposed configuration

TABLE I
ESD ENERGY CONVERSION EFFICIENCY AND DAILY SELF-DISCHARGE [12]

ESS	Efficiency	Daily self-discharge
Lead-acid	63 – 90%	0.033 – 1.10%
Lithium-ion	70 – 100%	0.03 – 0.33%
Super capacitor	65 – 99%	0.46 – 40%
Flywheel	70 – 96%	24 – 100%
Pumped Hydro.	65 – 87%	0%
Compressed Air.	57 – 89%	0%

To assess the overall efficiency of ESSs, not only the efficiency of ESDs must be considered, but also the efficiency of the interfacing power converter. Partial Power Converters (PPCs) have emerge as a higher

efficiency alternative to traditional DC-DC Full Power Converters (FPCs), in the former

only a part of the full system power is processed by the converter, reducing its size and losses compared to FPCs [13]. PPCs have been proposed for a broad variety of unidirectional power flow applications, such as PV power plants [13]–[15], long LED arrays [16] and electric vehicle fast charging stations [17]. This work proposes a novel bidirectional partial power converter topology, as an interface to connect a ESD to a grid-tied PV plant, in order to provide peak shaving capability. Lithium-ion batteries were chosen as the ESD to be applied, since they present the highest efficiency range and the lowest daily self-discharge rate (according to [12]).

CONFIGURATION & MATHEMATICAL MODELS

The proposed configuration is shown in Fig. 1, where a BESS is connected to the dc-link of a central inverter PV plant. The battery pack is interfaced, to the dc-link of the central inverter configuration, through 5 interleaved PPCs. Each PPC is formed by 8 semiconductors (MOSFETs), a transformer and an inductance, connected as shown in the figure. The central inverter configuration is composed by an array of several PV modules and a single 2 Level Voltage Source Inverter (2*LV SI*) connected to the grid. The mathematical model of PPC *j* (*j* = *{*1, . . . , 5*}*) is described by equations (1) to (6). The first 3 equations correspond to voltage dynamics, namely voltage across the

inductance *L* (*vLj*), voltage across the top winding and its semiconductors (*vfbpj*) and voltage in the bottom winding and its semiconductors (*vfbsj*). The latter 3 equations correspond to the current dynamics of PPC *j*, where *ixj*, *ibpj* and *ippcj*

correspond respectively to the current through inductance *L*, the bypass current and partial power converter current.The variables *mj* , *vx* and *vpv* represent respectively the modulation index of PPC *j* (*mj* $\in$ [0, 1]), the voltage in the terminals of the battery pack and the voltage across the dclink The parameters *n*1 and *n*2 correspond respectively to the number of turns in the primary (Fig. 1, top winding) and secondary (Fig. 1, bottom winding) of the transformer.

$$v_{Lj} = \left(\frac{n_2}{n_1+n_2}\right)\cdot v_{pv}\cdot m_j - v_x \quad (1)$$

$$v_{fbpj} = \left(\frac{n_1}{n_1+n_2}\right)\cdot v_{pv}\cdot m_j \quad (2)$$

$$v_{fbsj} = \left(\frac{n_2}{n_1+n_2}\right)\cdot v_{pv}\cdot m_j \quad (3)$$

$$i_{xj} = \frac{1}{s\cdot L}\left(\left(\frac{n_2}{n_1+n_2}\right)\cdot v_{pv}\cdot m_j - v_x\right) \quad (4)$$

$$i_{bpj} = \left(\frac{n_2}{n_1+n_2}\right)\cdot m_j\cdot i_{xj} \quad (5)$$

$$i_{ppcj} = \left(\frac{n_1}{n_1+n_2}\right)\cdot m_j\cdot i_{xj} \quad (6)$$

In order to increase the equivalent switching frequency and reduce the current ripple from and towards the battery pack and dc-link, 5 PPCs are interleaved and their PWM carriers

are shifted in $\varphi = 2\pi/n$, where *n* is the amount of interleaved

PPCs ($\varphi = 2\pi/5$ in this case).

The mathematical model of the 2*LV SI* grid currents in *dq* rotational reference frame (*igd* and *igq*), in

Laplace domain, is shown in equations (7) and (8). Where *Lg*, *Rg*, *ω*, *vrd*, *vrq*, *vgd* and *vgq* correspond respectively to the inductance and resistance of the filter, grid angular frequency, inverter voltages in *dq* rotational axes and grid voltages in *dq* rotational reference frame.

$$i_{gd} = \frac{1}{L_g \cdot s + R_g}\left(v_{rd} + L_g \cdot \omega \cdot i_{gq} - v_{gd}\right) \quad (7)$$

$$i_{gq} = \frac{1}{L_g \cdot s + R_g}\left(v_{rq} - L_g \cdot \omega \cdot i_{gd} - v_{gq}\right) \quad (8)$$

The mathematical model of the voltage across the dc-link capacitor *Cpv* (*vpv*) is shown in equation (9). Where *ipv*, *ibp*, *mu*, *mv*, *mw*, *igu*, *igv*, *igw* correspond to the PV plant output current, total bypass current (through all PPCs), modulation indexes per inverter phase and grid currents.

$$v_{pv} = \frac{1}{s \cdot C_{pv}}\left(i_{pv} + i_{bp} - m_u \cdot i_{gu} - m_v \cdot i_{gv} - m_w \cdot i_{gw}\right) \quad (9)$$

A. Partial Power Converters

In order for a power converter to be considered a PPC, the power processed by the converter must be lower than the input power. This relationship is called partial power ratio (*kpr*) and is mathematically represented by the ratio between the PPC processed power and its input power [16]. Therefore, a power converter must comply with $kpr < 1$ to be a PPC. Table II summarizes the equations governing the partiality of the proposed bidirectional PPC, for both power flow directions towards the BESS (noted by *bess*) and towards the dc-link (noted by *dc*).

Where *Gv* and η correspond respectively to the voltage gain and the efficiency of the converter.

TABLE II
PARTIALITY EQUATIONS

Power flow towards BESS	Power flow towards dc-link
$k_{pr\ bess} = \frac{v_x \cdot i_{ppc}}{v_{pv} \cdot i_{bp}}$	$k_{pr\ dc} = \frac{v_{pv} \cdot i_{bp}}{v_x \cdot i_{ppc}}$
$G_{v\ bess} = \frac{v_x}{v_{pv}}$	$G_{v\ dc} = \frac{v_{pv}}{v_x}$
$\eta_{bess} = G_{v\ bess} + k_{pr\ bess}$	$\eta_{dc} = \frac{G_{v\ dc} \cdot k_{pr\ dc}}{G_{v\ dc} + k_{pr\ dc}}$

B. Battery Energy Storage Sizing

A worst case scenario of providing 10% of the PV plant peak power (10% of 1*MW*) during t = 10 minutes was considered.

This time consideration corresponds to the available time for non-spinning reserves to respond after a contingency, having to be fully operational and able to provide 100% of its rated power to the electric network [18]. Hence, the BESS must be able to provide

$$E_{BESS} = \frac{10\% \cdot P_{pv\ mpp}}{1000 \cdot 60} \cdot t\,[kWh] = 17[kWh] \quad (10)$$

Where *Ppv mpp* is the maximum power the PV plant can generate and t is the time in minutes. Due to computational limitations the peak shaving effect provided by the BESS is analysed during short time

intervals, nevertheless the battery pack was designed to provide 100*kW* during 10 minutes.

CONTROL SCHEME

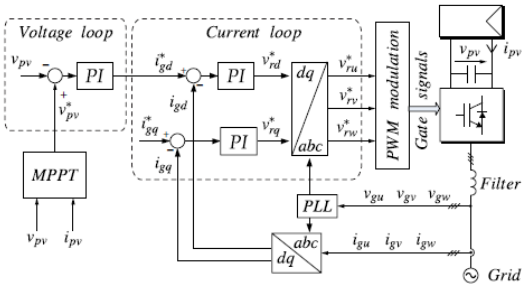

Fig. 2. Inversor control scheme

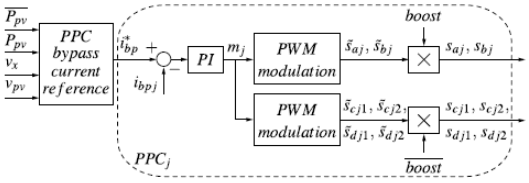

Fig. 3. Bidirectional PPC control scheme

A conventional Voltage Oriented Control (VOC) scheme, composed by an outer dc-link voltage loop and two inner current loops (direct igd and quadrature igq grid currents), is applied to the 2LV SI of the central inverter configuration as shown in Fig. 2. Where vrd and vrq correspond respectively to the direct and quadrature inverter voltages. The dc-link voltage reference v∗ paves is generated by a traditional Perturb and Observe (P&O) Maximum Power Point Tracking algorithm. Figure 3 shows the control scheme applied to each PPC. The leftmost block (PPC bypass current reference), which is explained through Fig. 4, generates the bypass current reference (i ∗ bp) for each interleaved PPC. A PI controller processes the error between i ∗ bp and the measurement of the bypass current in PPC j (ibpj), generating the modulation index, which is later passed to the PWM modulation block generating the signals s˜aj , s˜bj , s˜cj1, s˜cj2, s˜dj1 and s˜dj2.

FUZZY LOGIC CONTROLLER

Most of the real-world processes that require automatic control are non-linear in nature. That is, their parameter values alter as the operating point changes over time or both. In case of conventional control schemes, as they are linear, a controller can only be tuned to give good performance at a particular operating point or for a limited period of time. The controller needs to be retuned if the operating point changes with time. This necessity to retune has driven the need for adaptive controllers that can automatically retune themselves to match the current process characteristics. Analytical techniques may fail to give a precise solution in a controlling process. Where as an expert or a skilled human operator, without the knowledge of their underlying dynamics of a system can control a system more successfully. So it is worth simulating the controlling strategy based upon intuition and experience can be considered a heuristic decision or rule of thumb decision. This can be possible through the Fuzzy controller.

Fuzzy logic is an innovative technology that enhances conventional system design with engineering expertise. Using fuzzy logic, we can circumvent the need for rigorous mathematical modeling A human operator is far more successful in controlling a process than a controller designed by modern analytical technique. So it is worth simulating the control strategy based upon intuition and experience and can be considered as heuristic decision or rule of thumb decision. In academic and

technological arena, Fuzzy is a technical term that deals with ambiguity or vagueness based on human intuitions. Professor Lotfi A Zadeh introduced the concept of fuzzy sets, according to him. Fuzzy logic is a mathematical imprecise description.

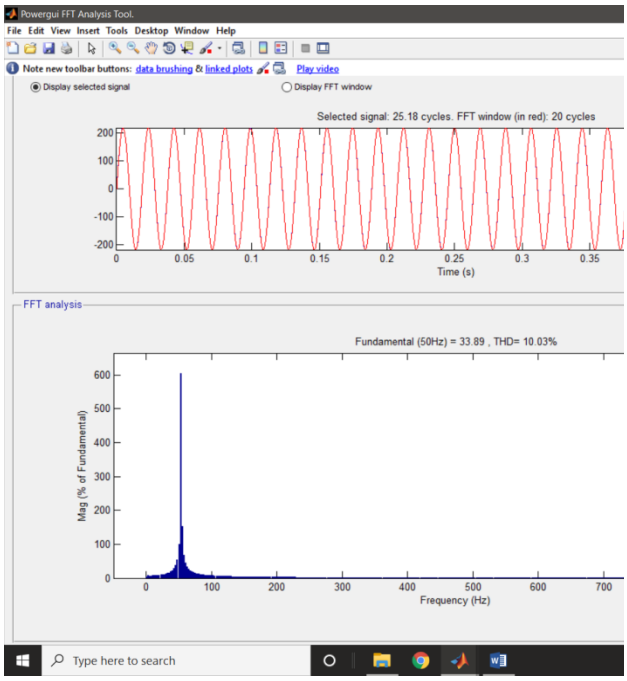

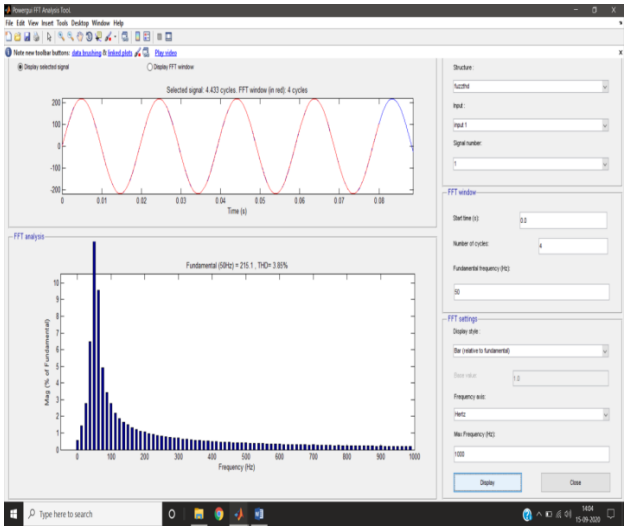

SIMULATION RESULTS

The circuital model of the full system was implemented in PLECS. Table shows the parameters applied in the simulation. A 1MW PV plant was considered, based on Canadian Solar CS6X-340M-FG PV modules, a tailored battery pack formed by muRata 6Ah LiB battery cells was considered.

CONFIGURATION PARAMETERS.

PV power plant (under STC conditions)		
Maximum power	$P_{pv\ mpp}$	$1\ MW$
Open circuit voltage	$v_{pv\ ocv}$	$970\ V$
Short circuit current	$i_{pv\ sc}$	$1327\ A$
Maximum power point voltage	$v_{pv\ mpp}$	$796\ V$
Maximum power point current	$i_{pv\ mpp}$	$1256\ A$
Modules connected in series	N_{sm}	21
Strings connected in parallel	N_{ps}	140
2LVSI & Grid		
PV 2LVSI dc-link capacitance	C_{pv}	$4400\ \mu F$
PV inverter dc-link voltage	v_{pv}	$740 - 1000\ V$
Grid voltage	$v_{ac\ RMS}$	$440\ V_{LL\ RMS}$
Grid inductance	L_g	$0.25\ mH$
Grid frequency	f_g	$50\ Hz$
Switching frequency	f_{sw}	$5\ kHz$
Battery pack		
Single cell capacity	C_{cell}	$6\ Ah$
Maximum cell discharge rate	$C_{rate\ out}$	$20\ C$
Maximum cell charge rate	$C_{rate\ in}$	$19\ C$
Number of cells	N_{cells}	1211
BESS maximum safety voltage	$\hat{v}_x$	$649\ V$
BESS minimum safety voltage	$\hat{v}_x$	$480\ V$
PPCs		
PPC inductance	L	$1\ mH$
PPC magnetising inductance	L_m	$1\ mH$
PPC transformer ratio	$n_1 : n_2$	$2:1$
Switching frequency	f_{bb}	$100\ kHz$
Sampling period	T_s	$1\ \mu s$

In order to validate the configuration two steps in solar irradiation were applied, while keeping temperature constant at

$25{\circ}C$. The first step consists in a step-down in solar irradiation from 1000 to $700W/m2$ at 0.5[s], the second step corresponds to a step-up from 700 to $1000W/m2$ at 1.3 [s].

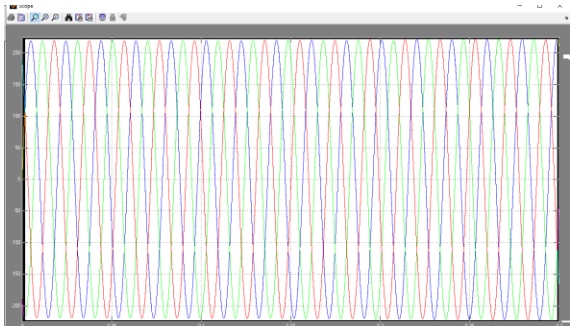

.

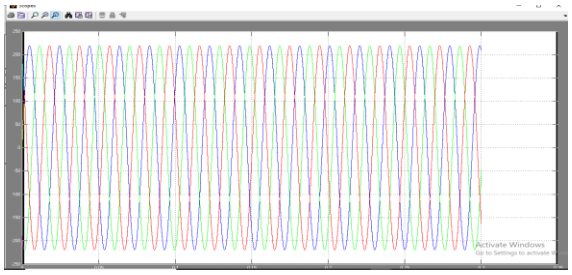

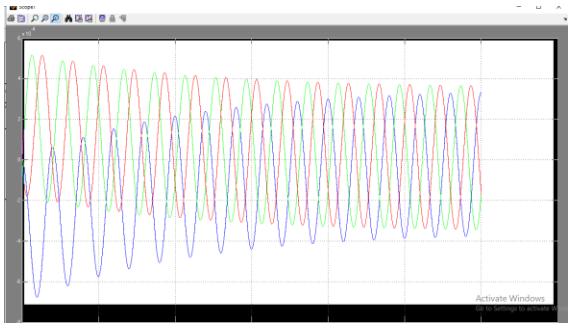

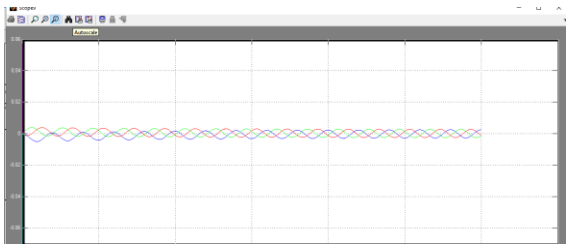

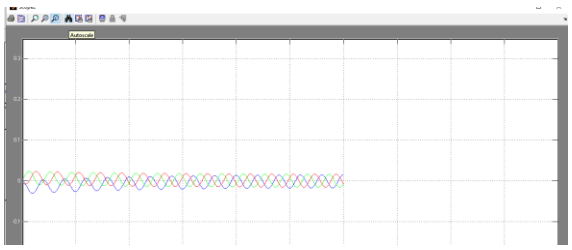

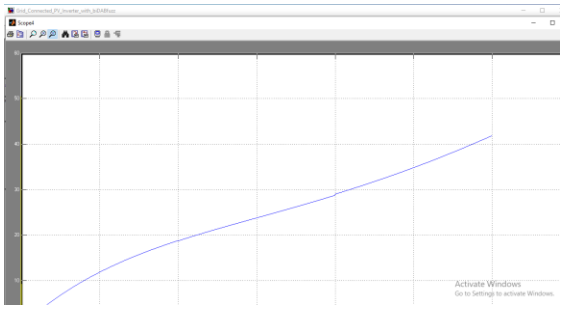

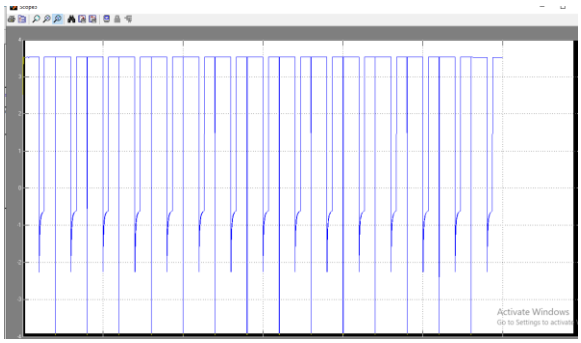

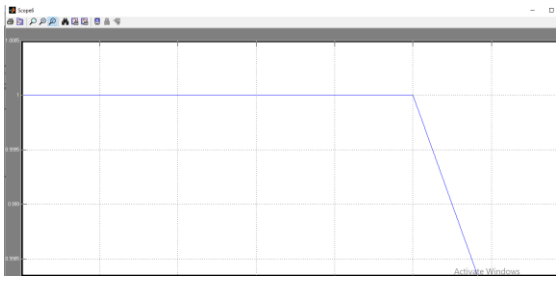

CONCLUSION

This paper presents a bidirectional PPC as an interface to merge a battery pack to a grid-tied PV plant, in order to provide peak shaving capability. The BESS enables the PV system to store (release) exceeding (lacking) PV power,providing peak shaved power to the grid. A full description and model of the system were given, providing a deeper understanding on how this bidirectional PPC operates. A tailored control strategy to manage the power flow between the battery pack and dc-link was tested, enabling the full system to inject peak shaved power to the grid. The standard P&O MPPT algorithm was able to

operate normally, even when power was being drawn or injected to the dc-link by the BESS. The proposed BESS configuration and control scheme were designed to be a plug-in solution for existing grid-tied PV plants, lacking peak shaving capability. Moreover, a small modification in the control strategy will allow BESS to mitigate (avoid) PV plants power curtailment, required by grid operators to compensate grid frequency variations. As a possible future work the authors propose the possibility to perform peak shaving and short term ancillary services without adding additional energy storage.

REFERENCES

[1] REN21, The First Decade 2004-2014 www.ren21.net. REN21, 2016.

[2] REN21, Renewable 2017 Global Status Report www.ren21.net. REN21, 2017.

[3] I. E. Commission et al., Grid Integration of Large-capacity Renewable Energy Sources and Use of Large-capacity Electrical Energy Storage: White Paper; October 2012. International Electro technical Commission, 2012.

[4] J. Widen, N. Carpman, V. Castellucci, D. Lingfors, J. Olauson, F. Re- ´ mouit, M. Bergkvist, M. Grabbe, and R. Waters, "Variability assessment and forecasting of renewable: A review for solar, wind, wave and tidal resources," Renewable and Sustainable Energy Reviews, vol. 44, pp. 356–375, 2015.

[5] M. N. Hjelmeland, C. T. Larsen, M. Korpas, and A. Helseth, "Provision ˚ of rotating reserves from wind power in a hydro-dominated power system," in Probabilistic Methods Applied to Power Systems (PMAPS), 2016 International Conference on. IEEE, 2016, pp. 1–7.

[6] J. Dong, F. Gao, X. Guan, Q. Zhai, and J. Wu, "Storage sizing with peak-shaving policy for wind farm based on cyclic markov chain model," IEEE Transactions on Sustainable Energy, vol. 8, no. 3, pp. 978–989, 2017.

[7] B.-R. Ke, T.-T. Ku, Y.-L. Ke, C.-Y. Chuang and H.-Z. Chen, "Sizing the battery energy storage system on a university campus with prediction of load and photovoltaic generation," IEEE Transactions on Industry Applications, vol. 52, no. 2, pp. 1136–1147, 2016.

[8] N. Muller, S. Kouro, H. Renaudineau, and P. Wheeler, "Energy storage ¨ system for global maximum power point tracking on central inverter pv plants," in Power Electronics Conference (SPEC), IEEE Annual Southern. IEEE, 2016, pp. 1–5.

[9] N. Muller, H. Renaudineau, F. Flores-Bahamonde, S. Kouro, and ¨ P. Wheeler, "Ultra capacitor storage enabled global mppt for photovoltaic central inverters," in Industrial Electronics (ISIE), 2017 IEEE 26th International Symposium on. IEEE, 2017, pp. 1046–1051.

[10] R. Sebastian, "Application of a battery energy storage for frequency ´ regulation and peak shaving in a wind diesel power system," IET Generation, Transmission & Distribution, vol. 10, no. 3, pp. 764–770, 2016.